

Simulation of electrical properties of $\text{In}_x\text{Al}_{1-x}\text{N}/\text{AlN}/\text{GaN}$ high electron mobility transistor structure*

Bi Yang(毕杨)^{1,†}, Wang Xiaoliang(王晓亮)^{1,2}, Xiao Hongling(肖红领)^{1,2},
Wang Cuimei(王翠梅)^{1,2}, Yang Cuibai(杨翠柏)^{1,2}, Peng Enchao(彭恩超)¹,
Lin Defeng(林德峰)¹, Feng Chun(冯春)^{1,2}, and Jiang Lijuan(姜丽娟)^{1,2}

¹Materials Science Center, Institute of Semiconductors, Chinese Academy of Sciences, Beijing 100083, China

²Key Laboratory of Semiconductor Materials Science, Institute of Semiconductors, Chinese Academy of Sciences, Beijing 100083, China

Abstract: Electrical properties of $\text{In}_x\text{Al}_{1-x}\text{N}/\text{AlN}/\text{GaN}$ structure are investigated by solving coupled Schrödinger and Poisson equations self-consistently. The variations in internal polarizations in $\text{In}_x\text{Al}_{1-x}\text{N}$ with indium contents are studied and the total polarization is zero when the indium content is 0.41. Our calculations show that the two-dimensional electron gas (2DEG) sheet density will decrease with increasing indium content. There is a critical thickness for AlN. The 2DEG sheet density will increase with $\text{In}_x\text{Al}_{1-x}\text{N}$ thickness when the AlN thickness is less than the critical value. However, once the AlN thickness becomes greater than the critical value, the 2DEG sheet density will decrease with increasing barrier thickness. The critical value of AlN is 2.8 nm for the lattice-matched $\text{In}_{0.18}\text{Al}_{0.82}\text{N}/\text{AlN}/\text{GaN}$ structure. Our calculations also show that the critical value decreases with increasing indium content.

Key words: GaN; InAlN; HEMT; 2DEG; polarization

DOI: 10.1088/1674-4926/32/8/083003

PACC: 7280E; 7125C; 7320D

1. Introduction

AlGaIn/GaN high-electron mobility transistors (HEMTs) have been intensively investigated due to their potential performance at high power and high frequency for commercial and military applications^[1–4]. In spite of the excellent device and circuit demonstrations, the lack of reliability still plagues the AlGaIn/GaN HEMTs^[5]. The reliability problems have been attributed to lattice defects introduced by the stress resulting from the mismatch and modulated by the piezoelectric effect^[6]. However, InAlN can be grown lattice matched to GaN when the indium content is about 0.17–0.18, reducing strain problems^[7] and potentially improving the reliability of the heterostructure. The lattice-matched $\text{In}_{0.18}\text{Al}_{0.82}\text{N}/\text{GaIn}$ HEMT, with negligible piezoelectric polarization, has much higher two-dimensional electron gas (2DEG) sheet density than that of a conventional AlGaIn/GaN HEMT due to the large spontaneous polarization^[8,9]. This enables thin-barrier structures to obtain high sheet charge density. Therefore, high-frequency characteristics of short-gate InAlN/GaN HEMTs can be significantly enhanced by suppressing the short channel effects^[10,11]. Although InAlN is difficult to grow, it has been intensively studied in recent years because of these promising capabilities^[12–15]. In these studies, an AlN interlayer is usually inserted between the InAlN and GaN layers to effectively reduce the alloy scattering and provide better confinement of electrons. However, the polarizations in $\text{In}_x\text{Al}_{1-x}\text{N}$

($0 \leq x \leq 1$) and the influence of AlN on the properties of the $\text{In}_x\text{Al}_{1-x}\text{N}/\text{AlN}/\text{GaIn}$ have not been investigated deeply in theory.

In this letter, the surface donor state^[16], the conduction band profile and electrostatic neutrality^[17] are considered when establishing the theory model. We will focus on the polarizations in $\text{In}_x\text{Al}_{1-x}\text{N}$ ($0 \leq x \leq 1$), as well as the electric fields induced by polarizations and sheet carriers in $\text{In}_x\text{Al}_{1-x}\text{N}/\text{AlN}/\text{GaIn}$ structure to investigate its band profile and 2DEG density by self-consistently solving coupled Schrödinger and Poisson equations. According to the calculations and analysis, the influence of the AlN interlayer on the properties of the $\text{In}_x\text{Al}_{1-x}\text{N}/\text{AlN}/\text{GaIn}$ HEMT structure has been discussed in detail.

2. Model and calculation

In our calculations, the InAlN barrier and AlN interlayer are supposed to be coherently grown on a thick GaN along [0001] with Ga (Al) polarity. AlN suffers from tensile strain because the lattice constant of AlN is smaller than that of GaN. When the indium composition is 0.18, the $\text{In}_{0.18}\text{Al}_{0.82}\text{N}$ is lattice matched to GaN and no stress is present. However, when it is smaller or larger than 0.18, InAlN will suffer from tensile or compressive strain^[18]. This is quite different from AlGaIn on a thick GaN, which always suffers from tensile strain and the di-

* Project supported by the Knowledge Innovation Engineering of the Chinese Academy of Sciences (No. YYYJ-0701-02), the National Natural Science Foundation of China (Nos. 60890193, 60906006), the State Key Development Program for Basic Research of China (Nos. 2006CB604905, 2010CB327503), and the Knowledge Innovation Program of the Chinese Academy of Sciences (Nos. ISCAS2008T01, ISCAS2009L01, ISCAS2009L02).

† Corresponding author. Email: ybi@semi.ac.cn

Received 28 February 2011, revised manuscript received 20 April 2011

© 2011 Chinese Institute of Electronics

rections of polarizations in AlGaIn are always from surface to substrate^[19]. The method of calculating the fixed polarization charge density at the nitride heterointerface has been discussed in detail^[20, 21]. It is supposed that the sheet carriers in the GaIn channel come from the surface donor state^[16]. The 2DEG sheet density N_{2D} can be obtained for an $\text{In}_x\text{Al}_{1-x}\text{N}/\text{AlN}/\text{GaIn}$ heterostructure according to conduction band profile and electrostatic neutrality,

$$\Delta E_{c(\text{AlN}/\text{GaIn})} + e \frac{\sigma_{\text{pAlN}} - N_{2D}}{\epsilon_{\text{AlN}}} d_{\text{AlN}} + e \frac{\sigma_{\text{pInAlN}} - N_{2D}}{\epsilon_{\text{InAlN}}} d_{\text{InAlN}} - \Delta E_{c(\text{AlN}/\text{InAlN})} = E_f + \phi_s, \quad (1)$$

where $\Delta E_{c(\text{AlN}/\text{GaIn})}$ is the conduction band offset between AlN and GaN, and $\Delta E_{c(\text{AlN}/\text{InAlN})}$ between AlN and InAlN, respectively; σ_{pAlN} and σ_{pInAlN} , both of which are set positive in our calculation for convenience, are the polarization-induced fixed charges at the AlN/GaN interface and InAlN surface, respectively; ϵ_{AlN} and ϵ_{InAlN} are the dielectric constants of AlN and InAlN; d_{AlN} and d_{InAlN} are the thicknesses of the AlN insertion layer and InAlN barrier layer; and ϕ_s is the depth of the Fermi level at the InAlN surface with respect to its conduction band edge.

The direction of electric field is set positive for convenience when it is from surface to substrate. For free electrons, the envelope wave function ψ_i and the i th subband energy E_i are given by the Schrödinger equation,

$$-\frac{\hbar^2}{2} \left[\frac{d}{dz} \left(\frac{1}{m^*} \frac{d\psi_i}{dz} \right) \right] + V(z) \psi_i = E_i \psi_i, \quad (2)$$

$$V(z) = V_h(z) + V_p(z) + V_{2D}(z), \quad (3)$$

where m^* is the effective mass of the electron, $V_h(z)$ is the conduction band edge potential function for the heterojunction structure, $V_p(z)$ is the potential induced by polarization charge, and $V_{2D}(z)$ is the electronic potential, which is related to the 2DEG distribution by the Poisson equation,

$$\frac{d}{dz} \left[\epsilon \frac{d}{dz} V_{2D}(z) \right] = -q N_{2D}(z). \quad (4)$$

Under equilibrium conditions, the distribution of the 2DEG in each subband obeys Fermi statistics, and the distribution of 2DEG is determined by

$$N_{2D}(z) = \sum_i \frac{m^* K T}{\pi \hbar^2} \ln \left[1 + \exp \frac{E_f - E_i}{K T} \right] |\psi_i(z)|^2, \quad (5)$$

where K is the Boltzmann constant and T is the temperature, which is set to 300 K in our calculation. The coupled Schrödinger and Poisson equations are solved using a self-consistent method.

3. Results and discussion

Firstly, we perform the calculations of the polarization of the $\text{In}_x\text{Al}_{1-x}\text{N}$ ($0 \leq x \leq 1$). In the absence of external electric fields, the total macroscopic polarization P of $\text{In}_x\text{Al}_{1-x}\text{N}$ is

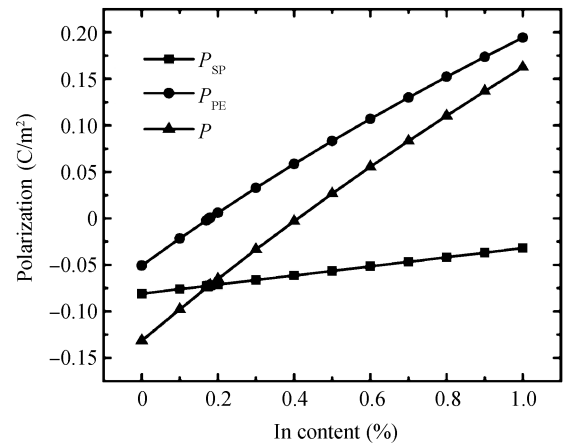


Fig. 1. Variations in spontaneous, piezoelectric and total polarization with indium content in $\text{In}_x\text{Al}_{1-x}\text{N}$ ($0 \leq x \leq 1$).

the sum of the spontaneous polarization P_{SP} and the piezoelectric polarization P_{PE} . The spontaneous polarization for InN, GaN and AlN was found to be negative^[22], meaning that the spontaneous polarization is pointing towards the substrate for Ga(Al)-face heterostructure. For $\text{In}_x\text{Al}_{1-x}\text{N}$ over the whole range of compositions, the piezoelectric polarization is negative for tensilely strained ($0 \leq x < 0.18$), zero for unstrained ($x = 0.18$) and positive for compressively strained barriers ($0.18 < x \leq 1$), respectively. Therefore, the alignment of the piezoelectric and spontaneous polarization is parallel in the case of tensilely strained, and antiparallel in the case of compressively strained top layers. The variations in spontaneous, piezoelectric and total polarization in $\text{In}_x\text{Al}_{1-x}\text{N}$ ($0 \leq x \leq 1$) with the indium content are shown in Fig. 1. The spontaneous polarization is always negative and decreases with increasing indium content. For the negative piezoelectric polarization ($0 \leq x < 0.18$), it also decreases with increasing indium content. However, when the piezoelectric polarization is positive ($0.18 < x \leq 1$), it increases with indium content. This makes the total polarization decrease and become zero at the composition of 0.41 (Fig. 1), which indicates that the piezoelectric polarization equals the spontaneous polarization. As the indium content increases over 0.41, the total polarization turns from negative to positive and increases with indium content.

The calculated 2DEG sheet density as a function of indium content for the $\text{In}_x\text{Al}_{1-x}\text{N}/\text{AlN}/\text{GaIn}$ heterostructure is shown in Fig. 2. The thicknesses of AlN and GaIn are set as 1 nm and 2 μm , respectively, and that of InAlN ranges from 8 to 20 nm. Our calculation shows that the 2DEG sheet density decreases almost linearly with increasing indium content. This trend is identical to that seen in experimental data^[8]. The distances between the curves in Fig. 2 decrease with increasing InAlN thickness. The curves nearly coincide with each other when the InAlN is thicker than 16 nm. According to the intercept on the abscissa of Fig. 2 for each barrier thickness by extrapolation, we determine that there is a threshold value of x above which no 2DEG is formed. On the basis of surface state theory^[16], the surface donor energy E_d drops below Fermi level E_F at the surface when x is greater than threshold value, preventing the surface donor states from being ionized and forming 2DEG.

The 2DEG sheet density in dependence on the

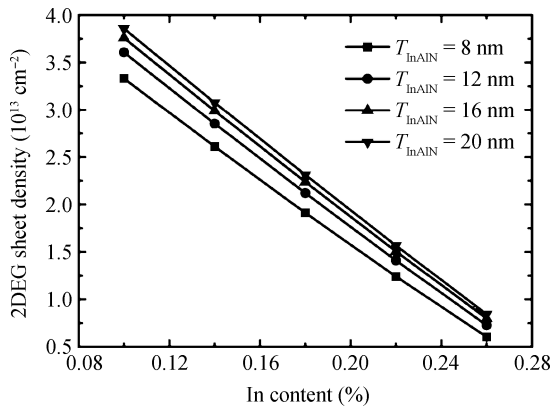


Fig. 2. Calculated 2DEG sheet density as a function of indium content for varying InAlN thickness at 300 K. The bottom curves denote thinner barriers and the upper curves thicker barriers. The structure is assumed to be undoped.

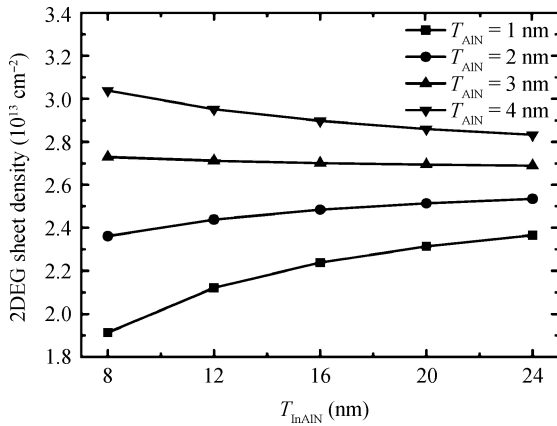


Fig. 3. The calculated 2DEG sheet density in dependence on the $\text{In}_{0.18}\text{Al}_{0.82}\text{N}$ barrier thickness for an $\text{In}_{0.18}\text{Al}_{0.82}\text{N}/\text{AlN}/\text{GaN}$ structure with different AlN thicknesses from 1.0 to 4.0 nm.

$\text{In}_{0.18}\text{Al}_{0.82}\text{N}$ thickness of an $\text{In}_{0.18}\text{Al}_{0.82}\text{N}/\text{AlN}/\text{GaN}$ heterostructure with different AlN thicknesses from 1 to 4 nm is shown in Fig. 3. When the AlN thickness is less than 2.0 nm, the 2DEG sheet density increases with $\text{In}_{0.18}\text{Al}_{0.82}\text{N}$ barrier thickness and tends to saturate. This tendency agrees with what has been reported in experiment^[18]. However, the dependence of the 2DEG sheet density on the barrier thickness tends to weaken with the increasing AlN thickness. When further increasing the AlN thickness to 3.0 nm, the 2DEG sheet density begins to decrease with increasing $\text{In}_{0.18}\text{Al}_{0.82}\text{N}$ thickness. This tendency is strengthened for an $\text{In}_{0.18}\text{Al}_{0.82}\text{N}/\text{AlN}/\text{GaN}$ heterostructure with a 4.0 nm AlN interlayer. It can be concluded from Fig. 3 that there should be a critical AlN thickness at which the 2DEG sheet density does not change with $\text{In}_{0.18}\text{Al}_{0.82}\text{N}$ thickness.

In order to confirm this claim, the calculated conduction band profiles and carrier distributions for an $\text{In}_{0.18}\text{Al}_{0.82}\text{N}$ (8 nm)/AlN/GaN ($2\ \mu\text{m}$) heterostructure with AlN interlayer thicknesses of 2 and 3 nm are shown in Fig. 4, in which z denotes the distance away from the surface to the inside of the heterostructure. There are two electric fields involved in GaN HEMT structures. One is E_p , induced by polarization and ex-

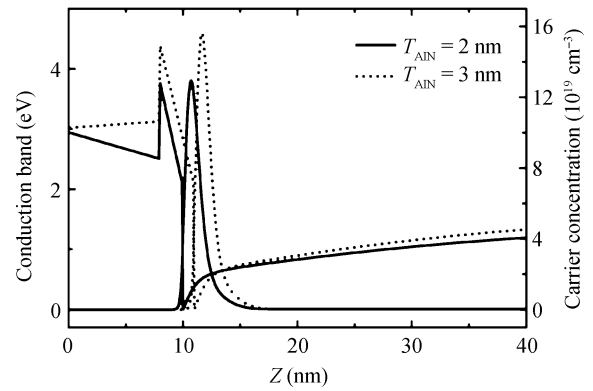


Fig. 4. Calculated conduction band profiles and carrier distributions for an $\text{In}_{0.18}\text{Al}_{0.82}\text{N}$ (8 nm)/AlN/GaN ($2\ \mu\text{m}$) heterostructure with the AlN interlayer thicknesses of 2 and 3 nm.

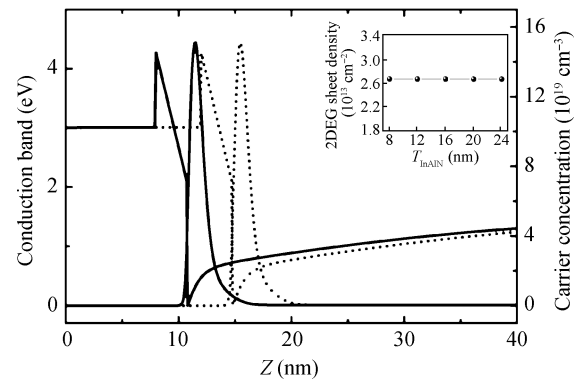


Fig. 5. Calculated conduction band profiles and carrier distributions for an $\text{In}_{0.18}\text{Al}_{0.82}\text{N}/\text{AlN}$ (2.8 nm)/GaN ($2\ \mu\text{m}$) heterostructure with the $\text{In}_{0.18}\text{Al}_{0.82}\text{N}$ thicknesses of 8 and 12 nm. The inserted graphics depict the variation in 2DEG sheet density as a function of the $\text{In}_{0.18}\text{Al}_{0.82}\text{N}$ thickness from 8 to 24 nm with 2.8 nm AlN.

pressed as $E_p = -\frac{\sigma_{p\text{InAlN}}}{\epsilon_{\text{InAlN}}}$. This points from the substrate towards the surface. The other one is $E_{2\text{DEG}}$, caused by sheet carriers in the GaN channel and expressed as $E_p = \frac{N_{2D}}{\epsilon_{\text{InAlN}}}$, and its direction is from surface to substrate. In the barrier layer, our calculation shows that the electric fields caused by polarization and sheet carriers are respectively $-495\ \text{MV}/\text{M}$ and $439\ \text{MV}/\text{M}$ when the AlN is 2 nm. The total electric field in $\text{In}_{0.18}\text{Al}_{0.82}\text{N}$ is $-56\ \text{MV}/\text{M}$ and its direction is from the substrate to the surface, making the band profile of the barrier layer lift up from the substrate to the surface. In this case^[16], E_d approaches and exceeds E_F with increasing barrier thickness, causing more surface donor states to be ionized and provide electrons for 2DEG. With the 3 nm AlN, the electric fields caused by polarization and sheet carriers are, respectively, $-495\ \text{MV}/\text{M}$ and $508\ \text{MV}/\text{M}$. The total electric field is $13\ \text{MV}/\text{M}$, enabling the conduction band profile of the barrier layer downward from the substrate to the surface, which is similar to the GaN cap layer^[23]. That leads to E_d dropping below E_F with the increasing barrier thickness^[16], resulting in fewer surface donors being ionized.

It can be seen in the inserted graphics in Fig. 5 that the 2DEG sheet density remains unchanged with different barrier thicknesses when the AlN thickness is 2.8 nm. Our calculation

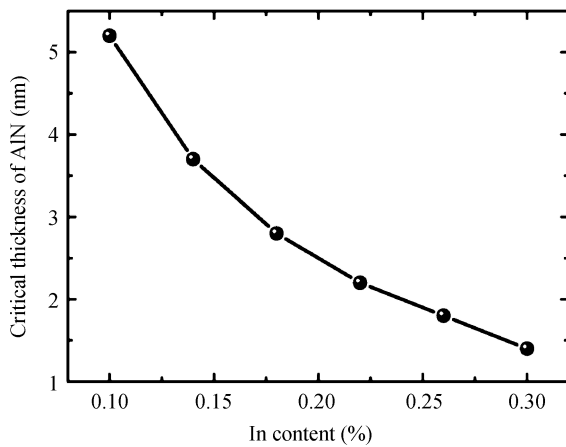


Fig. 6. Calculated critical thickness of AlN as a function of indium content in the $\text{In}_x\text{Al}_{1-x}\text{N}$ barrier layer.

shows that the electric field caused by polarization is equal to that caused by 2DEG at this critical thickness of AlN. Therefore, the total electric field is zero and the conduction band profile of $\text{In}_{0.18}\text{Al}_{0.82}\text{N}$ is horizontal (Fig. 5). Consequently, the location of E_d does not vary with the barrier thickness, resulting in a constant 2DEG sheet density.

The critical thickness of AlN largely depends on the indium content because the spontaneous and piezoelectric polarizations of the $\text{In}_x\text{Al}_{1-x}\text{N}$ barrier layer are strongly modulated by it (Fig. 1). As can be seen in Fig. 3, the 2DEG sheet density and $E_{2\text{DEG}}$ increase with the AlN thickness. Therefore, the critical AlN thickness decreases with increasing indium content (Fig. 6). The 2DEG sheet density decreases or increases with increasing $\text{In}_x\text{Al}_{1-x}\text{N}$ barrier thickness when the AlN thickness is greater or less than the critical value. A similar phenomenon for the AlGaIn/AlN/GaN structure has been reported by Kong *et al.*^[24]. A series of experiments will be carried out in order to investigate in depth the InAlN/AlN/GaN structure. Relevant data will be published later.

4. Conclusions

In summary, the electrical properties of $\text{In}_x\text{Al}_{1-x}\text{N}/\text{AlN}/\text{GaN}$ structure have been investigated by solving coupled Schrödinger and Poisson equations. The relationship between internal polarizations in $\text{In}_x\text{Al}_{1-x}\text{N}$ and indium contents has been discussed. The 2DEG sheet density will decrease with increasing indium content. The dependence of conduction band profile on the electric fields in InAlN is studied in detail. Our calculations show that there is a critical thickness of AlN in $\text{In}_x\text{Al}_{1-x}\text{N}/\text{AlN}/\text{GaN}$ structure. The 2DEG sheet density will increase with the $\text{In}_x\text{Al}_{1-x}\text{N}$ thickness when the AlN thickness is less than the critical value. However, when the AlN thickness is greater than the critical value, the 2DEG sheet density will decrease with increasing barrier thickness. The reasons for this phenomenon have been discussed. It is also suggested by our calculations that the critical value decreases with increasing indium content. These calculations may provide a guideline for the epilayer structure optimization of $\text{In}_x\text{Al}_{1-x}\text{N}/\text{AlN}/\text{GaN}$ HEMTs.

References

- [1] Poblencz C, Corrion A L, Recht F, et al. Power performance of AlGaIn/GaN HEMTs grown on SiC by ammonia-MBE at 4 and 10 GHz. *IEEE Electron Device Lett*, 2007, 28: 945
- [2] Palacios T, Chakraborty A, Rajan S, et al. High-power AlGaIn/GaN HEMTs for Ka-band applications. *IEEE Electron Device Lett*, 2005, 26: 781
- [3] Wu Y F, Saxler A, Moore M, et al. 30-W/mm GaN HEMTs by field plate optimization. *IEEE Electron Device Lett*, 2004, 25: 117
- [4] Higashiwaki M, Mimura T, Matsui T. AlGaIn/GaN heterostructure field-effect transistors on 4H-SiC substrates with current-gain cutoff frequency of 190 GHz. *Appl Phys Express*, 2008, 1: 021103
- [5] Medjdoub F, Carlin J F, Gonschorek M, et al. Can InAlN/GaN be an alternative to high power/high temperature AlGaIn/GaN devices. *International Electron Devices Meeting*, 2006: 673
- [6] Joh J, Alamo J del. Mechanisms for electrical degradation of GaN high-electron mobility transistors. *International Electron Devices Meeting*, 2006: 1
- [7] Kuzmik J. InAlN/(In)GaIn high electron mobility transistors: some aspects of the quantum well heterostructure proposal. *Semicond Sci Technol*, 2002, 17: 540
- [8] Gonschorek M, Carlin J, Feltn E, et al. Two-dimensional electron gas density in AlInN/AlN/GaN heterostructures. *J Appl Phys*, 2008, 103: 093714
- [9] Hiroki M, Maeda N, Kobayashi T. Fabrication of an InAlN/AlGaIn/AlN/GaN heterostructure with a flat surface and high electron mobility. *Appl Phys Express*, 2008, 1: 111102
- [10] Crespo A, Bellot M, Chabak K, et al. High-power Ka-band performance of AlInN/GaN HEMT with 9.8-nm-thin barrier. *IEEE Electron Device Lett*, 2009, 31: 2
- [11] Sun H, Alt A, Benedickter H, et al. 100-nm-gate (Al, In) N/GaN HEMTs grown on SiC with $f_T = 144$ GHz. *IEEE Electron Device Lett*, 2010, 31: 293
- [12] Butté R, Carlin J, Feltn E, et al. Current status of AlInN layers lattice-matched to GaN for photonics and electronics. *J Phys D: Appl Phys*, 2007, 40: 6328
- [13] Gonschorek M, Carlin J, Feltn E, et al. High electron mobility lattice-matched AlInN/GaN field-effect transistor heterostructures. *Appl Phys Lett*, 89, 2006: 062106
- [14] Jeganathan K, Shimizu M, Okumura H, et al. Lattice-matched InAlN/GaN two-dimensional electron gas with high mobility and sheet carrier density by plasma-assisted molecular beam epitaxy. *J Cryst Growth*, 2007, 304: 342
- [15] Xie J, Ni X, Wu M, et al. High electron mobility in nearly lattice-matched AlInN/AlN/GaN heterostructure field effect transistors. *Appl Phys Lett*, 2007, 91: 132116
- [16] Jogai B. Influence of surface states on the two-dimensional electron gas in AlGaIn/GaN heterojunction field-effect transistors. *J Appl Phys*, 2003, 93: 1631
- [17] Asbeck P M, Yu E T, Lau S S, et al. Piezoelectric charge densities in AlGaIn/GaN HFETs. *Electron Lett*, 1997, 33: 1230
- [18] Medjdoub F, Carlin J, Gaquiere C, et al. Status of the emerging InAlN/GaN power HEMT technology. *Open Electrical and Electronic Engineering Journal*, 2008, 2: 1
- [19] Ambacher O, Smart J, Shealy J R, et al. Two-dimensional electron gases induced by spontaneous and piezoelectric polarization charges in N- and Ga-face AlGaIn/GaN heterostructures. *J Appl Phys*, 1999, 85: 3222
- [20] Guo L C, Wang X L, Xiao H L, et al. The influence of internal electric fields on the transition energy of InGaIn/GaN quantum

- well. *J Cryst Growth*, 2007, 298: 522
- [21] Kuzmik J. InAlN/(In) GaN high electron mobility transistors: some aspects of the quantum well heterostructure proposal. *Semicond Sci Technol*, 2002, 17: 540
- [22] Bernardini F, Fiorentini V, Vanderbilt D. Spontaneous polarization and piezoelectric constants of III–V nitrides. *Phys Rev B*, 1997, 56: 10024
- [23] Smorchkova I P, Chen L, Mates T, et al. AlN/GaN and (Al,Ga)N/AlN/GaN two-dimensional electron gas structures grown by plasma-assisted molecular-beam epitaxy. *J Appl Phys*, 2001, 90: 5196
- [24] Kong Y C, Zheng Y D, Zhou C H, et al. Two-dimensional electron gas densities in AlGaN/AlN/GaN heterostructures. *Appl Phys A: Mater*, 2006, 84: 95